Science Advances
AAAS

advances.sciencemag.org/cgi/content/full/6/6/eaaz2736/DC1

Supplementary Materials for

Small-molecule activation of lysosomal TRP channels ameliorates Duchenne muscular dystrophy in mouse models

Lu Yu, Xiaoli Zhang, Yexin Yang, Dan Li, Kaiyuan Tang, Zifan Zhao, Wanwan He, Ce Wang, Nirakar Sahoo, Kimber Converso-Baran, Carol S. Davis, Susan V. Brooks, Anne Bigot, Raul Calvo, Natalia J. Martinez, Noel Southall, Xin Hu, Juan Marugan, Marc Ferrer, Haoxing Xu*

*Corresponding author. Email: haoxingx@umich.edu

Published 7 February 2020, *Sci. Adv.* **6**, eaaz2736 (2020)
DOI: 10.1126/sciadv.aaz2736

This PDF file includes:

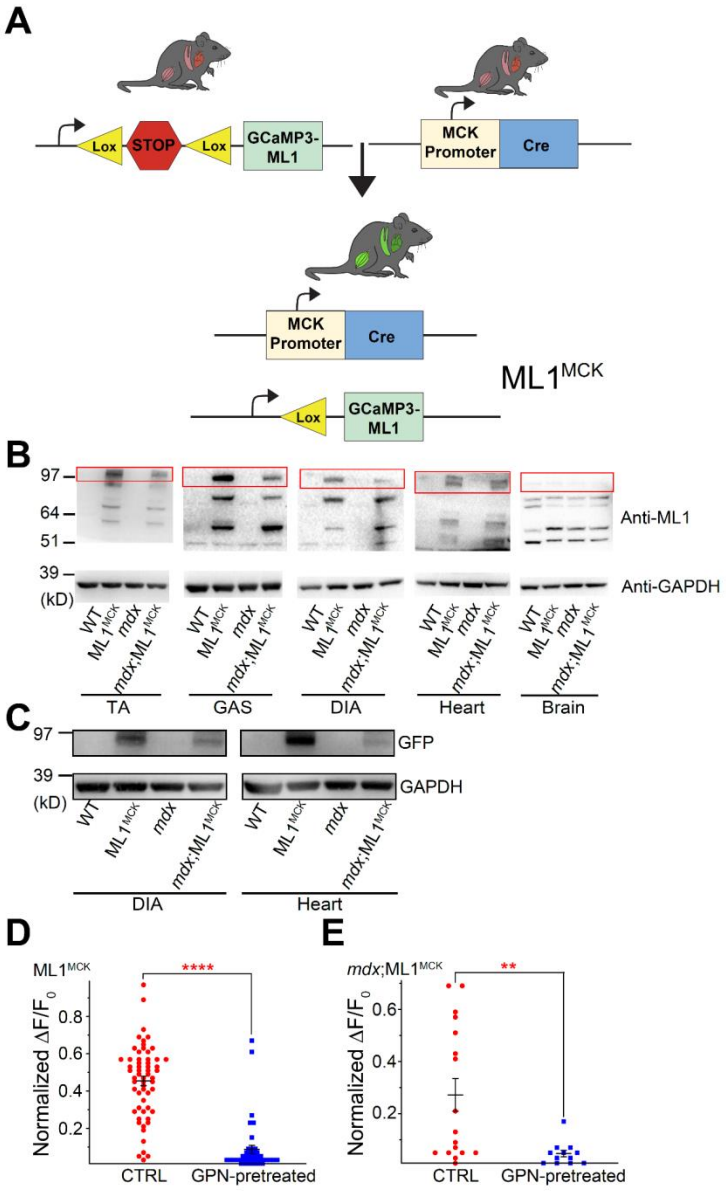

Fig. S1. Muscle-specific transgenic overexpression of ML1. (**A**) The GCaMP3-ML1 transgene was inserted into the ROSA26 locus with a *lox*STOP*lox* cassette. The transgenic mice were crossed with MCK-Cre mice to achieve muscle-specific overexpression of ML1. (**B**) Source files for Fig. 1B showing western blotting with anti-ML1 antibody in brain and various skeletal muscle tissues, including GAS, TA, and DIA from WT, ML1 *ROSA-lSl*;MCK Cre (ML1^{MCK}), *mdx*, and *mdx*; ML1^{MCK} mice. Note that the tissue-specific proteolytic cleavage products of full-length GCaMP3-ML1 were also recognized by an anti-GFP antibody, which can be used to detect GCaMP proteins (*15*). (**C**) Western blotting analysis of GCaMP3-ML1 expression in ML1^{MCK} DIA and cardiac muscle with anti-GFP antibody. (**D**, **E**) Quantification of lysosomal Ca^{2+} release from ML1^{MCK} and *mdx*;ML1^{MCK} myotubes (see **Fig. 1H**, **I**). All data are means ± s.e.m.; $^{**}p < 0.01$; $^{****}p < 0.0001$.

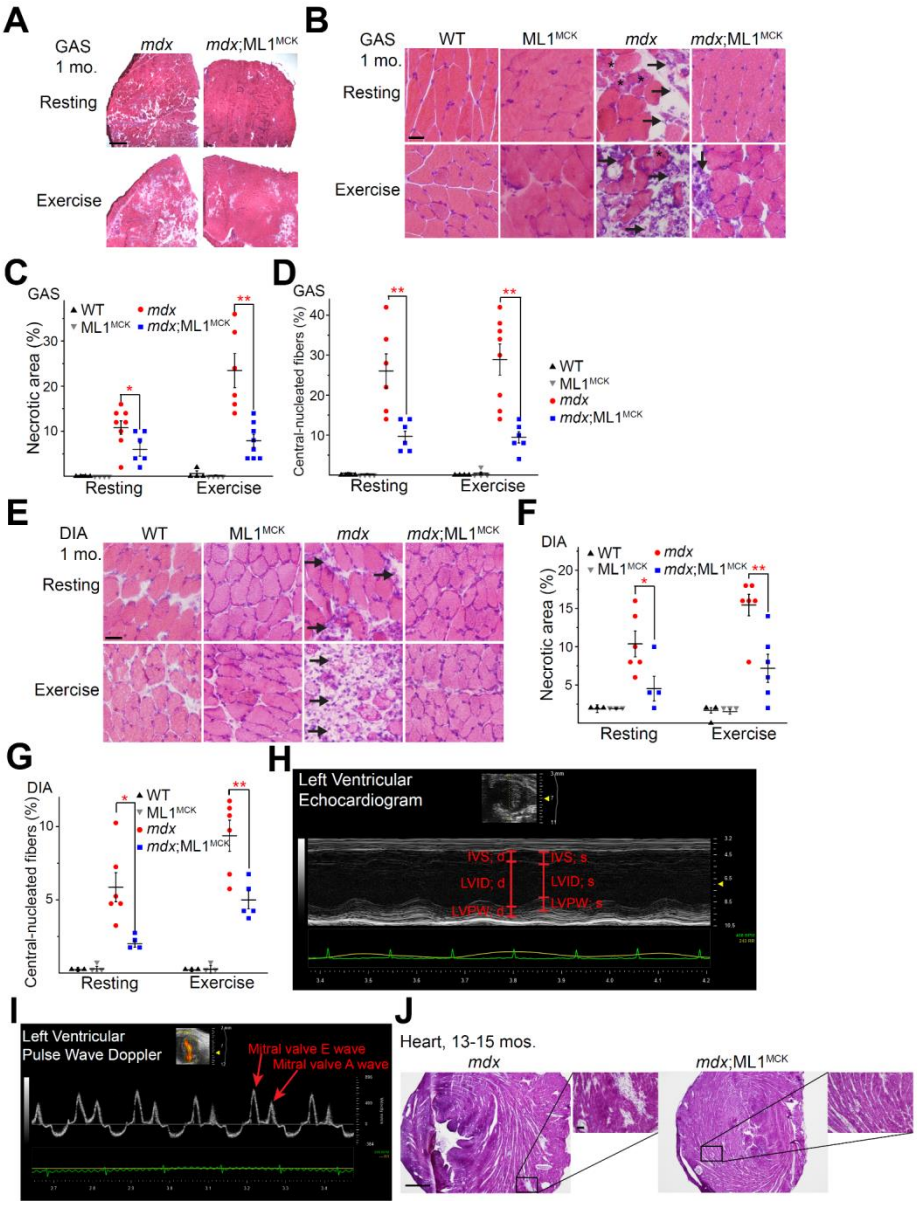

Fig. S2. Muscle-specific transgenic overexpression of ML1 reduces GAS, DIA, and cardiac pathologies in *mdx* mice. (**A**, **B**) H&E staining of GAS from 1-month-old *mdx* and *mdx*;ML1^{MCK} mice under low (A) and high (B) magnification. Scale = 500 μm (A) or 50 μm (B). Both male and female mice were used. (**C**, **D**) Quantification of necrosis (C) and central-nucleation (D) of representative H&E stained images as shown in A and B. Each datum (n indicates the number of the muscle) represents the averaged result from at least three representative images randomly selected from at least three sections. Statistical analyses were performed by experimenters who were blind to animal genotypes. (**E**) H&E staining of DIA. Scale = 50 μm. (**F**, **G**) Quantification of necrotic and central-nucleated fibers as shown in E. (**H**) A diagram demonstrating how the left ventricle echocardiograph was performed and quantified. IVS: interventricular septum; d: diastole; s: systole; LVID: left ventricular internal diameter; LVPW: left ventricular posterior wall. (**I**) Mitral valve E and A waves were measured by left ventricular Pulse wave (PW) Doppler. (**J**) H&E staining of cardiac muscle sections from 15 months old *mdx* and *mdx*;ML1^{MCK} mice. Only male *mdx* mice were used for echocardiography, but both male and female mice were included in the histology analysis. Scale = 500 μm (low magnification) or 50 μm (high magnification). All data are means ± s.e.m.; *p < 0.05, **p < 0.01.

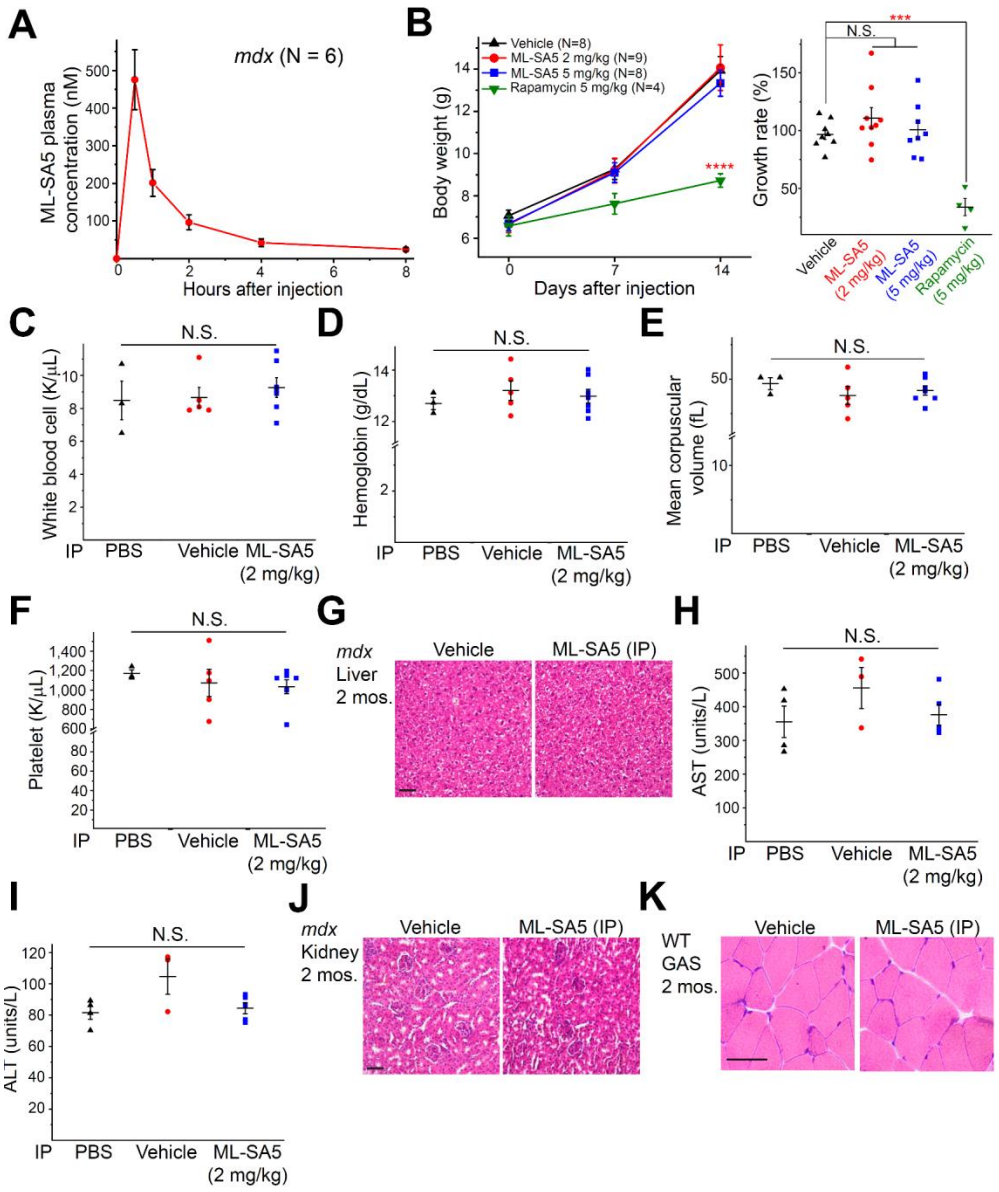

Fig. S3. Pharmacokinetics and toxicity of ML-SA5. (**A**) Plasma concentrations of ML-SA5 at different time points (0, 0.5, 1, 2, 4, and 8h) following i.p. injection (5 mg/kg) into *mdx* mice (N = 6 animals). (**B**) Effects of i.p. injection of ML-SA5 and rapamycin on animal body weight. N indicates the number of tested animals in each group. Growth rate = (weight after injection – weight before injection) / weight before injection. (**C-F**) Complete blood count for white blood cells (C), hemoglobin (D), mean corpuscular volume (E), and platelets (F). Blood was collected from PBS-, vehicle-, and ML-SA5 (2 mg/kg)-injected *mdx* mice at the age of 2 mos.. Daily injection started from P14. Both male and female mice were randomly assigned into different treatment groups. (**G**) Liver histology of vehicle- and ML-SA5-injected *mdx* mice. (**H**, **I**) Liver biochemistry measuring the levels of serum aspartate aminotransferase (AST, H) and alanine aminotransferase (ALT, I). Serum was collected from *mdx* mice at the age of 2 mos.. (**J**) Kidney histology of vehicle- and ML-SA5-injected *mdx* mice. (**K**) Effects of ML-SA5 (2 mg/kg) i.p. injection on muscle histology in WT mice. All data are mean ± s.e.m.; ***$p < 0.001$.

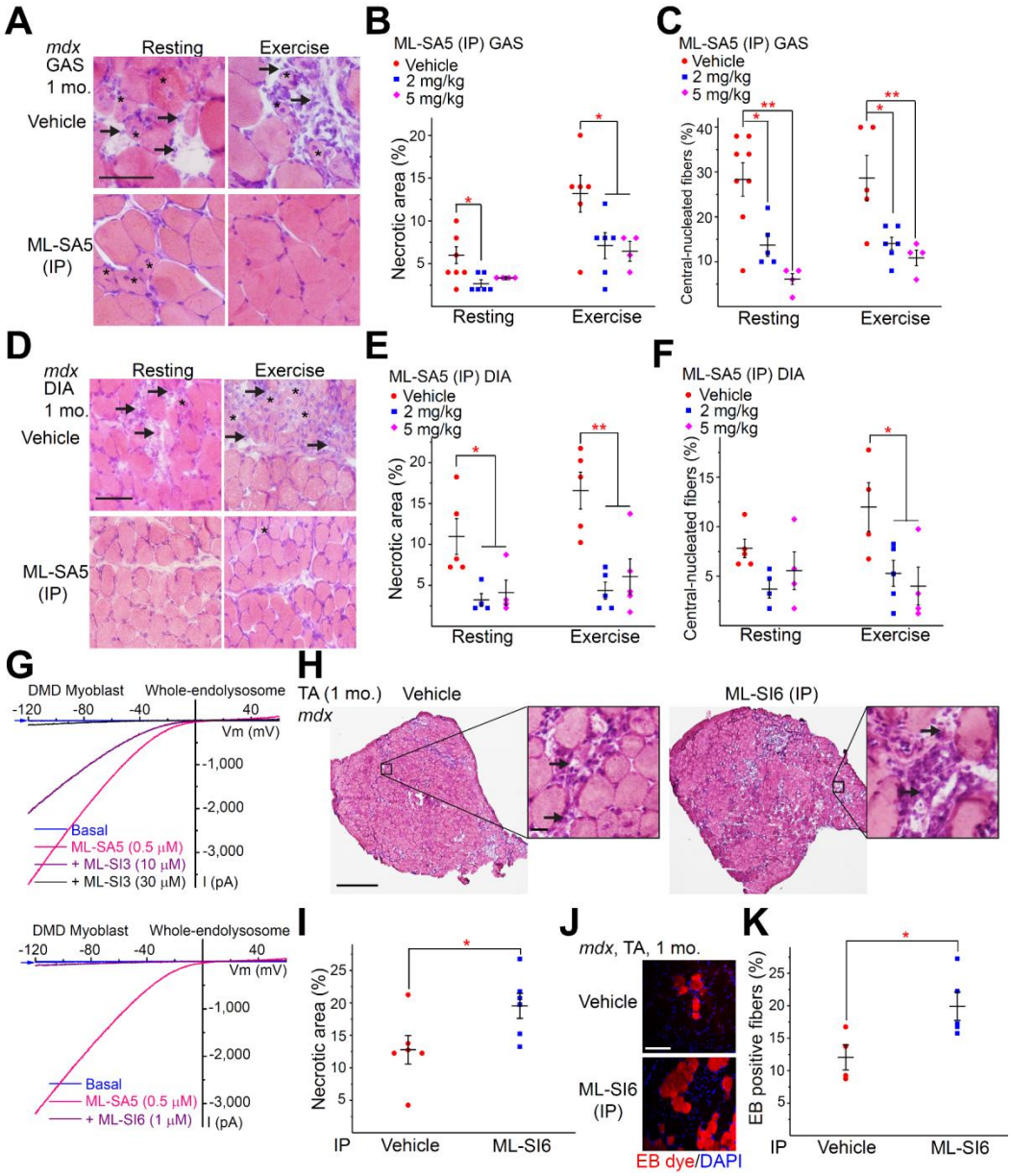

Fig. S4. ML1 agonist injection (intraperitoneal) ameliorates GAS and DIA pathologies in *mdx* mice. (**A**) H&E staining of GAS from mice given daily i.p. injection of ML-SA5 (2 mg/kg) for 14 d. Scale bar = 50 μm. (**B**, **C**) Quantification of necrotic (B) and centrally-nucleated fibers (C) in ML-SA5-injected GAS. (**D**-**F**) H&E staining of DIA from ML-SA5-injected *mdx* mice. Scale bar = 50 μm. (**G**) ML-SA5 (0.5 μM)-activated whole-endolysosome ML1 currents were sensitive to the synthetic inhibitors of ML1, ML-SI3 (10, 30 μM), and ML-SI6 (1 μM) in DMD myoblasts. (**H**) H&E staining of TA from 1-month-old *mdx* mice given daily i.p. injection of ML-SI6 (2 mg/kg) for 14 d. Scale = 500 μm or 20 μm (zoom in images). (**I**) Quantification of necrotic area of sections in H. (**J**, **K**) EB dye uptake in TA from ML-SI6-injected *mdx* mice. Scale = 100 μm. Male and female mice were randomly assigned to different treatment groups in experiments shown in this figure. All data are mean ± s.e.m.; **p* < 0.05, and ***p* < 0.01.

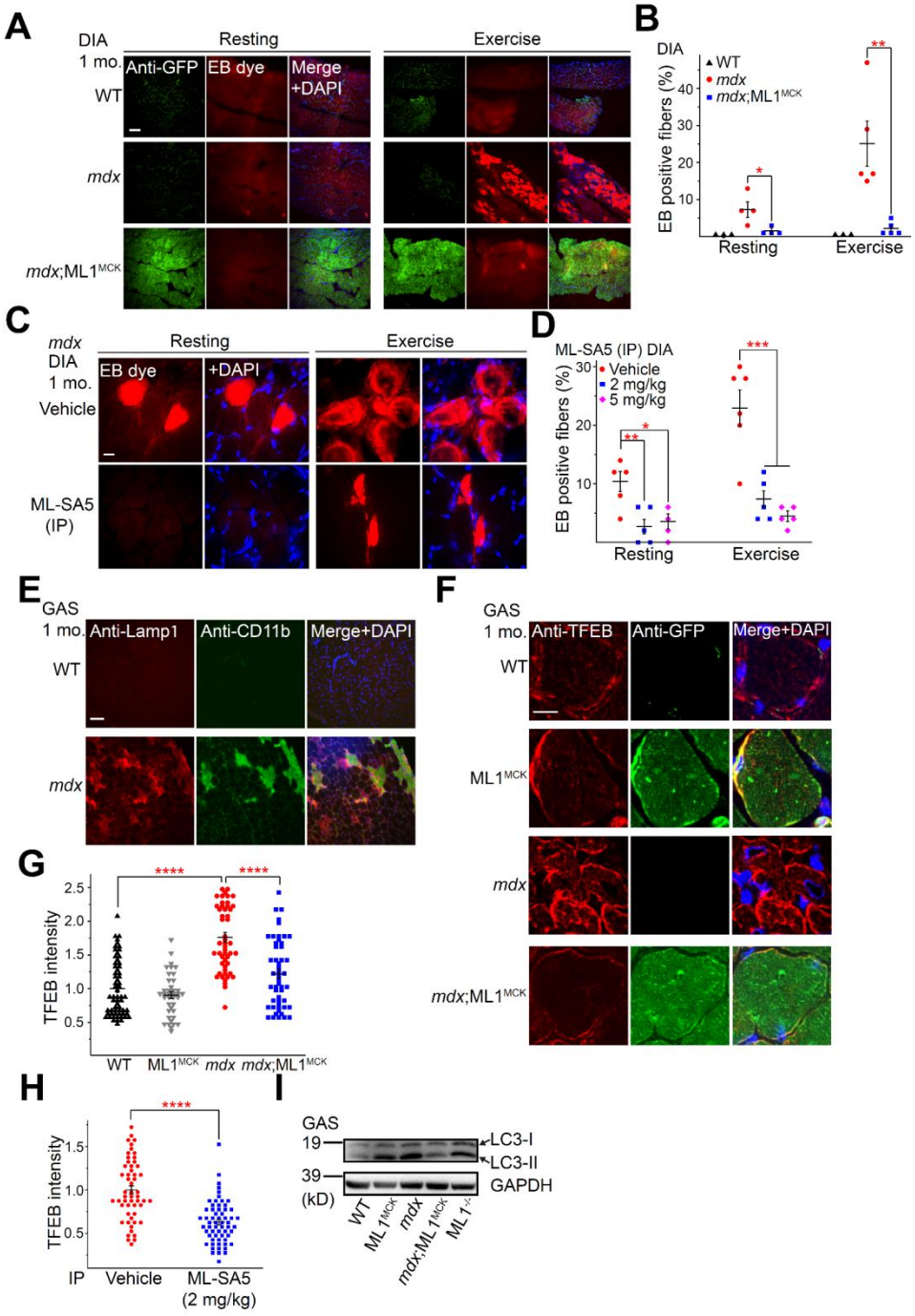

Fig. S5. Activation of ML1 corrects lysosomal insufficiency and improves sarcolemmal repair in *mdx* mice. (**A**, **B**) Transgenic overexpression of ML1 decreased EB dye uptake in DIA from *mdx* mice at the age of 1 mo.. Scale = 100 μm. (**C**, **D**) ML-SA5 (2, 5 mg/kg) treatment decreased EB-positive fibers before and after treadmill exercise. Scale = 10 μm. (**E**) Lamp1 expression was high in CD11b-positive macrophages. Scale bar = 100 μm. (**F**, **G**) TFEB immunolabeling in GAS from WT, ML1^{MCK}, *mdx*, and *mdx*;ML1^{MCK} mice. Scale bar = 10 μm. Each datum represents one muscle fiber in randomly selected images from at least four animals in each group. (**H**) Treatment of 2 mg/kg ML-SA5 for 14 d decreased TFEB intensity (see Fig. 6G). (**I**) Western blotting analysis of LC3-II expression levels in GAS from various transgenic mice. Both male and female mice were used. All data are means ± s.e.m.; *$p < 0.05$, **$p < 0.01$, ***$p < 0.001$, and ****$p < 0.0001$.

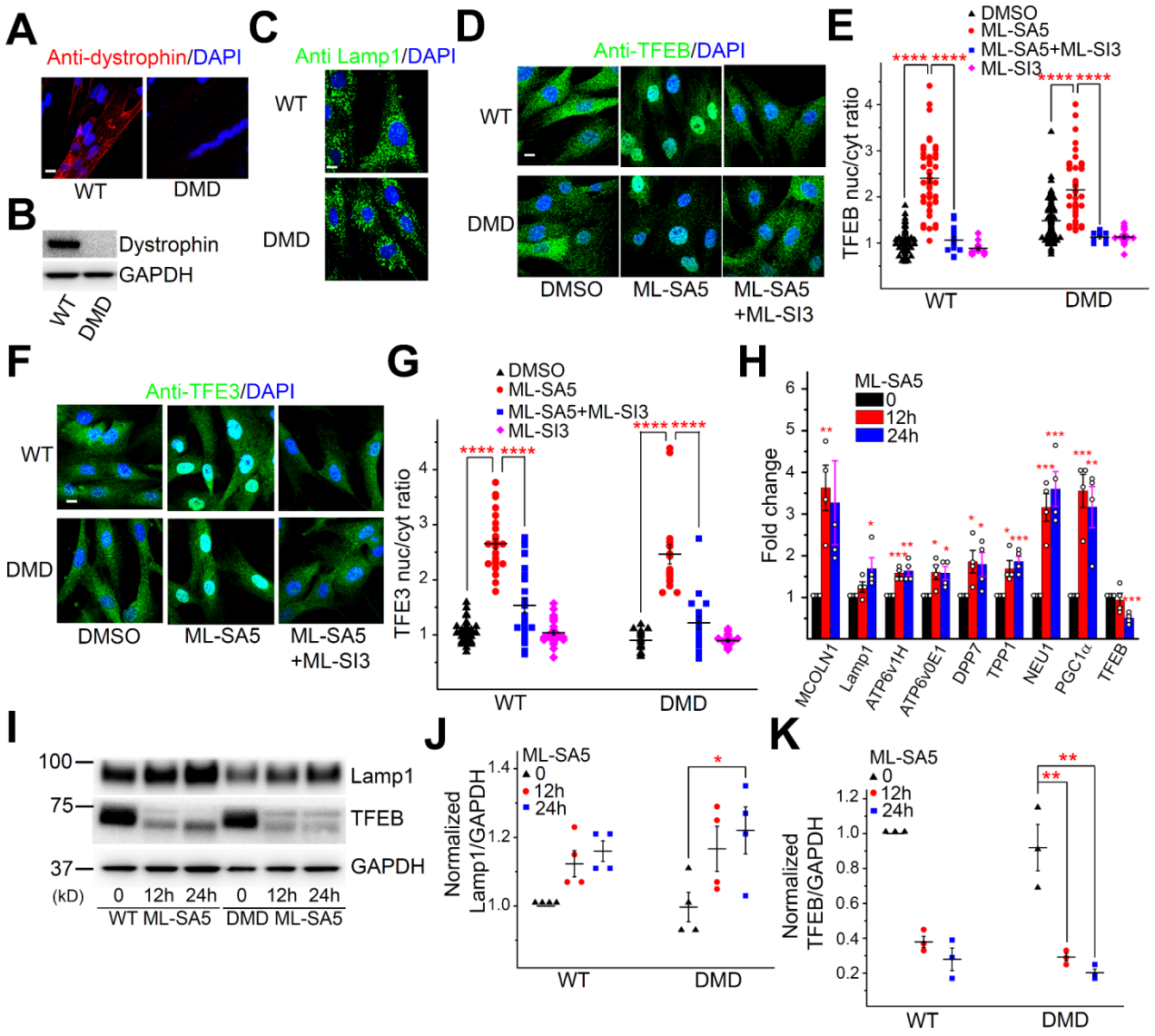

Fig. S6. ML1 agonist activates TFEB/TFE3 and lysosomal biogenesis in DMD myoblasts. (**A**) Dystrophin immunolabeling in myotubes differentiated from immortalized WT and DMD human myoblasts. Scale bar = 10 μm. (**B**) Western blotting analysis of dystrophin expression in WT and DMD myoblasts. (**C**) Lamp1 immunostaining in WT and DMD cells after ML-SA5 (0.5 μM) treatment. Scale bar = 10 μm. (**D**) TFEB immunolabeling of WT and DMD myoblasts upon ML-SA5 (0.5 μM) and ML-SI3 (20 μM) treatment. Scale = 10 μm. (**E**) Quantification of TFEB fluorescence intensity in nucleus divided by that in cytosol. (**F**, **G**) Images (F) and quantification (G) for TFE3 immunolabeling of WT and DMD myoblasts upon ML-SA5 (0.5 μM) and ML-SI3 (20 μM) treatment. Scale = 10 μm. (**H**) mRNA expression levels of TFEB target genes determined by qPCR. HPRT was used as a control. (**I-K**) Lamp1 and TFEB protein levels in WT and DMD myoblasts were increased and decreased, respectively, upon ML-SA5 (0.5 μM) treatment for 12 h and 24 h. All data are means ± s.e.m.; *$p < 0.05$, **$p < 0.01$, and ****$p < 0.0001$.

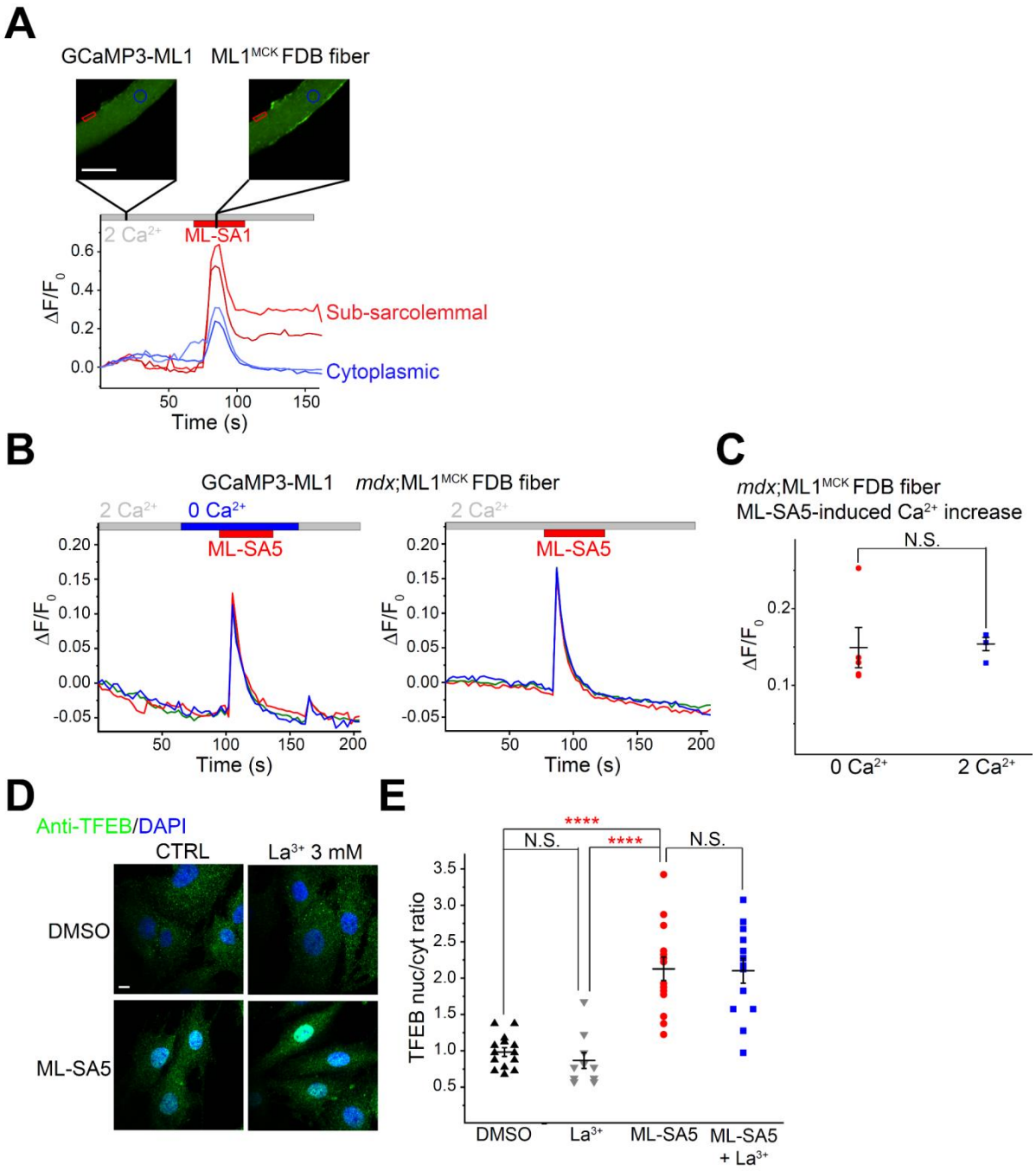

Fig. S7. Sarcolemmal Ca^{2+} entry is not required for ML-SA–induced TFEB nuclear translocation. (**A**) GCaMP3 Ca^{2+} imaging studies of isolated FDB single fibers from $ML1^{MCK}$ mice. ML-SA1 (30 μM) induced Ca^{2+} increases in both sub-sarcolemmal regions (red) and cytoplasm (blue). Note that Lamp1-positive lysosomes are known to accumulate in the sub-sarcolemmal regions as well. Scale = 50 μm. (**B**) ML-SA5-induced Ca^{2+} responses in *mdx*;$ML1^{MCK}$ FDB single fibers in 0 *vs.* 2 mM Ca^{2+} Tyrode's solutions. (**C**) Quantification for ML-SA5-induced Ca^{2+} increase in 0 *vs.* 2 mM Ca^{2+} solutions in *mdx*;$ML1^{MCK}$ FDB fibers. (**D**) ML-SA5 induced TFEB nuclear translocation in the presence of 3 mM La^{3+}, a membrane-impermeable TRPML blocker. Scale bar = 10 μm. (**E**) Quantification for TFEB fluorescence intensity from D. All data are means ± s.e.m.; ****$p < 0.0001$.

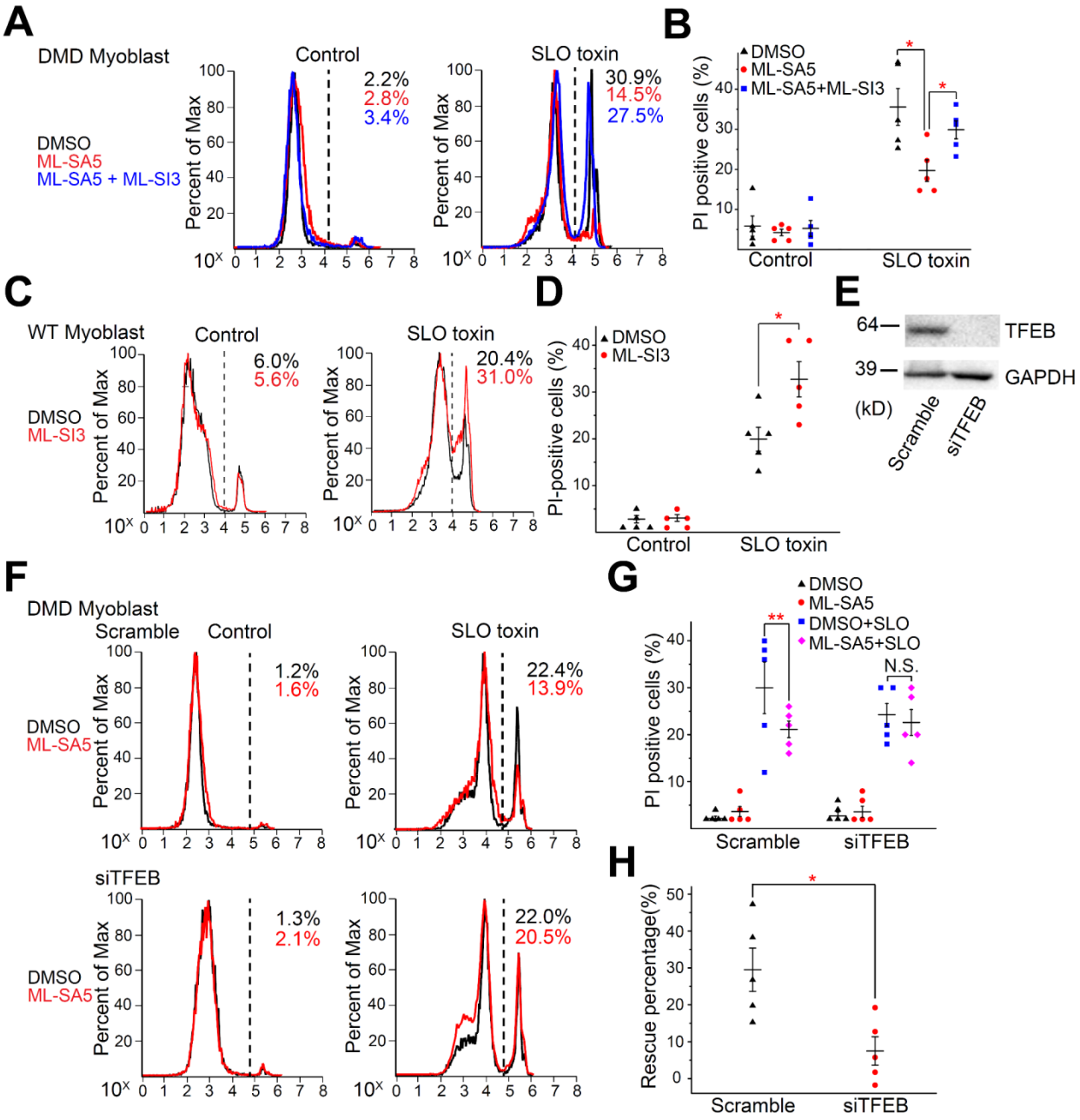

Fig. S8. ML1 agonist prevents cell death in DMD myoblasts via TFEB. (**A**) Flow cytometric analysis of the viability of cultured muscle cells, assayed by PI staining following SLO toxin-induced membrane damage. Human DMD myoblasts were pre-treated with ML-SA5 (0.5 μM) and ML-SI3 (20 μM) for 7 h before being subjected to SLO toxin (0.5–1 μg/ml, 10 min) challenge. (**B**) Quantification of five independent repeats as shown in A. (**C**, **D**) PI-staining-based flow cytometry of the viability of cultured WT myoblasts pretreated with ML-SI3 (20 μM) upon membrane damage by SLO toxin. (**E**) TFEB-specific siRNA decreased TFEB protein expression in DMD cells. (**F-H**) TFEB knockdown by siRNA blocked ML-SA5 effects on cell survival. Rescue percentage is calculated by the difference between the percentages of DMSO- and ML-SA5-treated cell death induced by SLO challenge divided by the percentage of DMSO-treated, SLO-induced cell death. All data are means ± s.e.m.; *$p < 0.05$, and **$p < 0.01$.

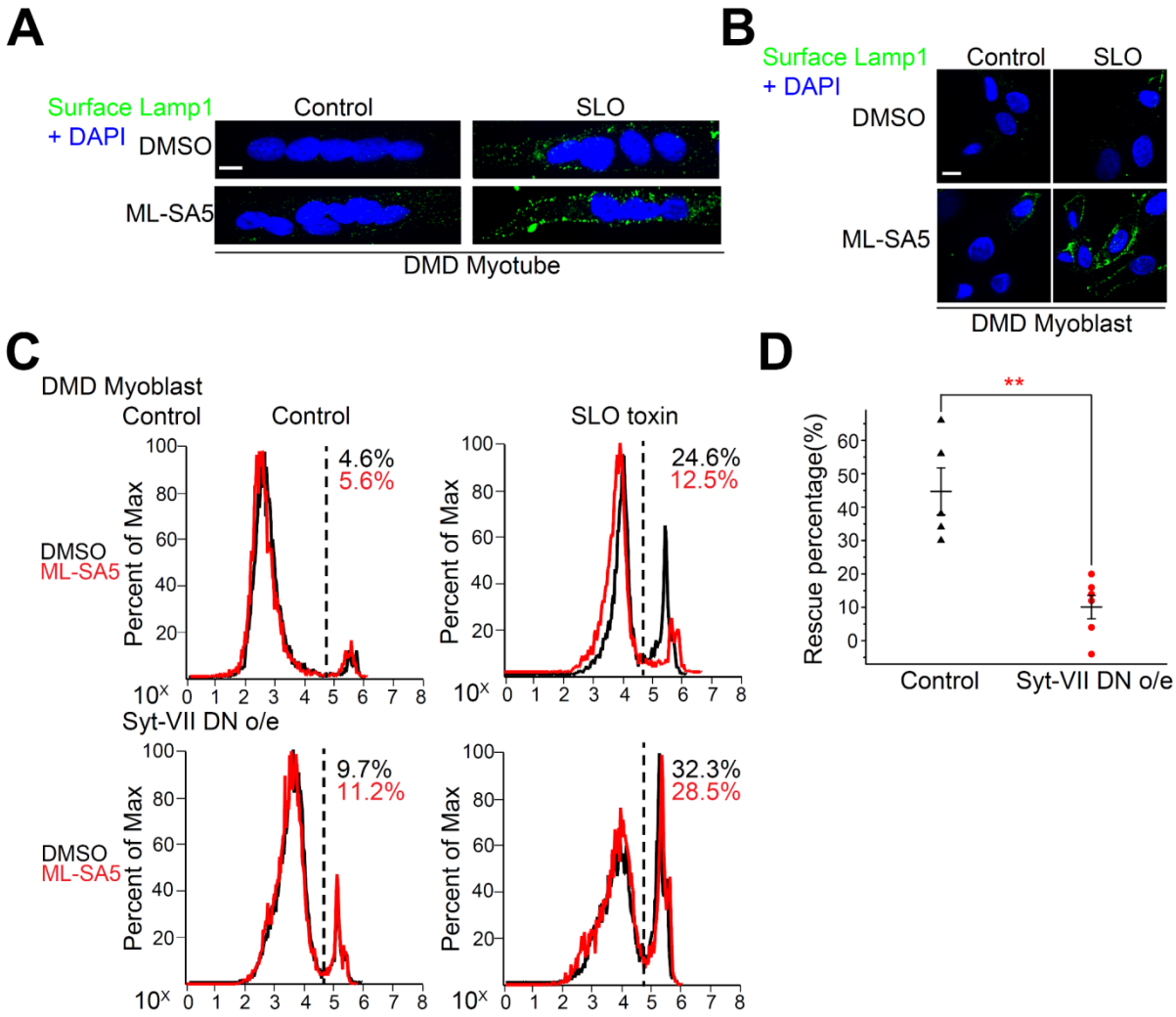

Fig. S9. Lysosomal exocytosis is required for ML-SA5–induced sarcolemma repair and cell survival. (**A**, **B**) Lamp1 surface immunolabeling of DMD differentiated myotubes (A) and myoblasts (B) after ML-SA5 (0.5 μM) pretreatment and SLO (1 μg/mL, 30 min) challenge. Surface expression of Lamp1 was assayed with an anti-Lamp1 antibody that recognizes a luminal epitope in non-permeabilized cells. Scale = 10 μm. (**C**, **D**) Flow cytometric analysis of DMD myoblasts transfected with a Syt-VII dominant-negative construct to block lysosomal exocytosis. DMD differentiated myotubes were pre-treated with ML-SA5 (0.5 μM) and challenged with SLO (1 μg/mL, 30 min). Data are means ± s.e.m.; $^{**}p < 0.01$.

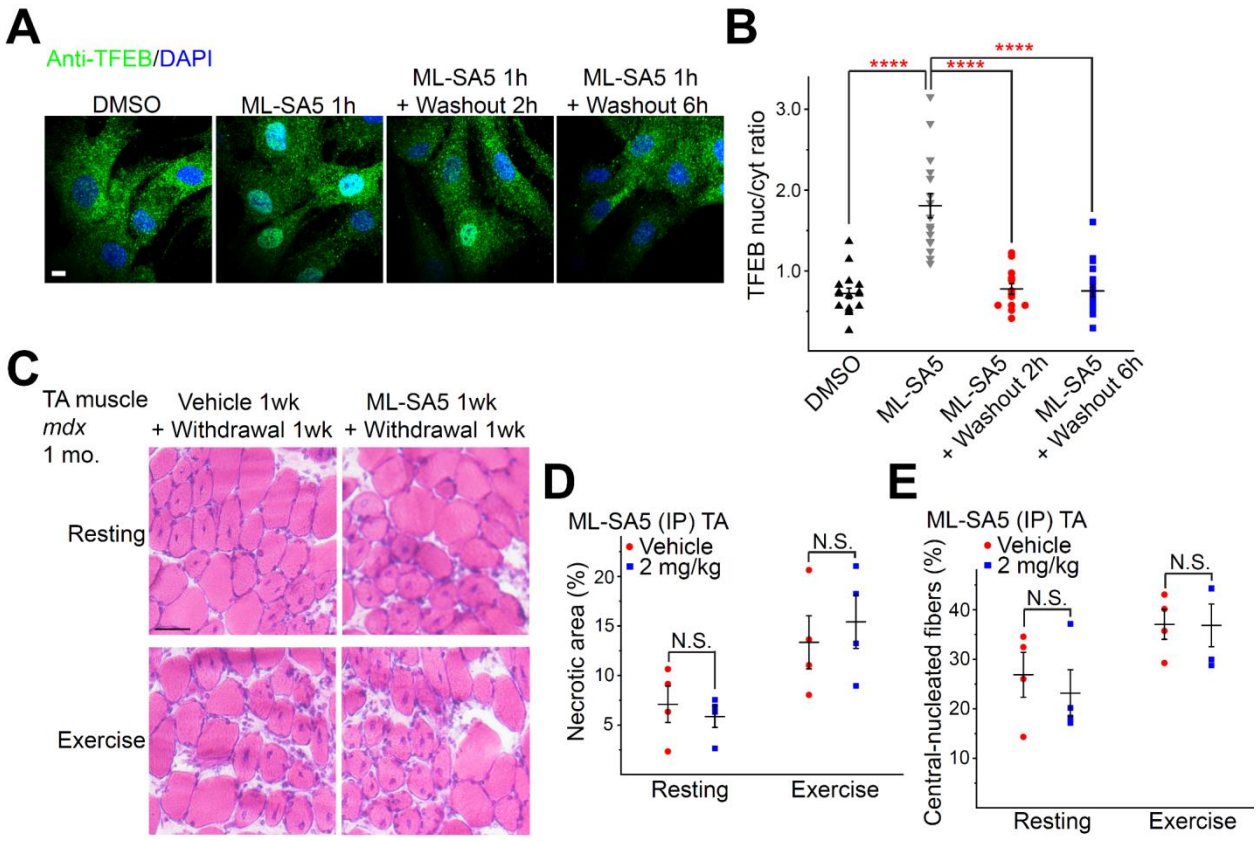

Fig. S10. Requirement of continuous agonist administration in achieving muscle protective effects. (**A**, **B**) The effects of ML-SA5 washout on TFEB nuclear translocation. Scale = 10 μm. (**C**) H&E staining of TA muscle sections from *mdx* mice that were treated with ML-SA5 at P14 for one week followed by drug withdrawal for another week. Mice were sacrificed at the age of 1 mo.. (**D**, **E**) Quantifications of necrotic area (D) and central-nucleation (E) in the muscle sections shown in C. All data are means ± s.e.m.; ****$p < 0.0001$.